Pergamon

J. Biomechanics, Vol. 28, No. 2, pp. 173–186, 1995

0021–9290/95 $9.50 + 0.00

0021–9290(94)E0040-A

LUMBAR SPINE MAXIMUM EFFORTS AND MUSCLE RECRUITMENT PATTERNS PREDICTED BY A MODEL WITH MULTIJOINT MUSCLES AND JOINTS WITH STIFFNESS

Ian A. F. Stokes and Mack Gardner-Morse

University of Vermont, Department of Orthopaedics and Rehabilitation, Burlington, VT 05405, U.S.A.

Abstract—The transmission of load through the lumbar spine was analyzed in a model of the five lumbar vertebrae, the sacrum/pelvis and the thorax, and 66 symmetric pairs of multijoint muscles. The model was used to test the hypotheses that (1) the need to maintain equilibrium simultaneously at all vertebral levels precludes simultaneous maximum activation of synergistic muscles and (2) that the maximum loads which could be carried by the spine and the degree of muscle activation increases with increasing motion segment stiffness. Maximum moments applied to T12 were calculated for moments in three principal directions, subject to equilibrium at all six joints and to constraints on the maximum muscle stress and intervertebral displacements.

A model with realistic motion segment stiffness predicted maximum efforts between 1.4 and 3.3 times greater than a model with 'ball-and-socket' joints, and in better agreement with published results from maximum effort experiments. The differences in maximal effort were greater than the moments transmitted through the joints. While muscle activation levels were greater, many synergistic muscles were still submaximally activated. Antagonistic muscles were recruited to maintain multijoint equilibrium. We concluded that (1) muscle activations permitted in single anatomic level analyses are generally not compatible with equilibrium at other levels; (2) the effect of moment transmission in the joints gives a more realistic representation of the lumbar spine.

INTRODUCTION

Analyses of load transmission through the lumbar spine are complicated because the spine anatomy includes many joints, and has many muscles which cross several of these joints. Most previous biomechanical analyses of the spine (Andersson and Winters, 1990; Andres and Chaffin, 1991; Ladin *et al.*, 1991; McGill, 1992; Morris *et al.*, 1961; Schultz, 1990) have been done with a free body diagram created by a single transverse cutting plane through one vertebral level (usually L3–L4). Such analyses ignore the requirement that equilibrium must be satisfied simultaneously at all the articulations, and do not consider the implications of multijoint muscles.

Even with these simplifications, there is still a redundant number of unknown forces in the analyses. This redundancy problem is usually solved by grouping muscles into 'equivalent' muscles and then using muscle forces and/or joint forces in the cost function of an optimization problem (Andersson and Winters, 1990; Schultz, 1990). Such models generally underestimate synergistic and antagonistic muscle activity compared to findings of EMG experiments (Lavender *et al.*, 1992a, b; Schultz, *et al.*, 1982), particularly for loading conditions which are asymmetric with respect to the sagittal plane (Schultz *et al.*, 1982; Seroussi and Pope, 1987).

Received in final form 2 *April* 1994.

Most models also assume that the motion segment can transmit forces, but do not permit moment transmission. Because the way in which forces are transmitted through the motion segments *in vivo* are not exactly known (Wilder *et al.*, 1989), generally an arbitrary point has been taken in these analyses to represent the center of force action through the disc.

Not all models make all of these assumptions. There have been several attempts to develop three-dimensional models of the spine. Cheng and Kumar (1991) considered the equilibrium of several two-dimensional spinal levels sequentially. Yettram and Jackman (1982) looked at changes in spinal forces with posture. Wynarsky and Schultz (1991) used a three-dimensional model to study optimal correction of spinal deformity. Bergmark (1989) and Dietrich *et al.* (1990) both used three-dimensional models to examine the structural stability of the resulting solutions. However, three-dimensional models of the lumbar spine with multijoint muscles have not previously been used to analyze lumbar spinal muscle recruitment and loading at all of the lumbar joints simultaneously.

This study used a three-dimensional lumbar spine model with realistic anatomy in which equilibrium had to be satisfied simultaneously at all the joints crossed by multijoint muscles. Since motion segments are complex flexible structures, both the forces and moments associated with their deformations were included in the model.

The purpose of this article is to determine consequences of the fact that most muscles of the spine cross

multiple articulations, and to demonstrate the effects of motion segment stiffness on the magnitude of maximum efforts and on the associated patterns of muscle activation. Maximum moments applied to T12 were calculated in the three principal directions, subject to equilibrium at all six joints and constraints on the maximum muscle stress and intervertebral displacements. The model was used to test the hypotheses that (1) the need to maintain equilibrium simultaneously at all vertebral levels precludes simultaneous maximum activation of synergistic muscles and (2) that the maximum loads which could be carried by the spine and the degree of muscle activation increases with increasing motion segment stiffness.

METHODS

A three-dimensional lumbar spine model was constructed using available published data for the positions of the vertebrae, the attachments and sizes of 66 symmetric multijoint muscle pairs, and the properties of spinal motion segments (Fig. 1). Two different models with the same geometry (vertebral positions, locations of muscle attachment points and physiological cross sectional area) were used to compare two different motion segment representations. The motion segments were represented as either beams having published stiffness properties, referred to as the *stiffness model*, or as simple 'ball-and-socket' joints between the vertebrae, referred to as the *static model* (Fig. 2). These models were used to determine maximal load transmission through the spine with the requirement that muscle forces be compatible with equilibrium at all six joints of the lumbar spine.

The model included the five lumbar vertebrae, considered as rigid bodies, and two further rigid bodies representing the thorax and the sacrum/pelvis (Fig. 3). The positions of vertebrae L1–L5 and the attachment of 49 symmetric extensor muscle pairs were digitized from the figures given in Bogduk *et al.* (1992a). For certain thoracic fibers shown by Bogduk *et al.* (1992a) as having a curved region close to their insertions, the muscle force was considered to be aligned with the straight part of the muscle path. The physiological cross sectional area (PCSA) of each muscle was also taken from Bogduk *et al.* (1992a). An additional five muscle pairs beyond those specified by Bogduk *et al.* (1992a) were added to represent the thoracic multifidi that attach in the lumbar region. The thoracic multifidi were assumed to be morphologically similar to the lumbar multifidi (Bogduk, 1993).

The attachments and PCSA of the psoas major muscles were obtained from Bogduk *et al.* (1992b). The psoas muscles which attach to the intervertebral disc were assumed to act equally between the superior and inferior vertebra. The PCSA values were weighted by the prevalence of the particular slip when it was not present in all specimens studied by Bogduk *et al.* (1992b). One muscle pair was added to represent the rectus abdominis with the cross sectional area taken from Reid and Costigan (1985) and attachment points were measured from an anatomic specimen. The pelvis/sacrum was fully constrained in the model (no movement was permitted). The geometry represented a spine in a neutral standing position. It was assumed that no forces or moments (due to bodyweight or elastic stresses) were present. The positions of the vertebrae centers, and details of the muscle anatomy are given in Appendix A.

Two simplifying assumptions about the muscles were made: (1) All muscles were assumed to take a straight line path from origin to insertion. Most dorsal fascicles (multifidus, iliocostalis, and longissimus) are known to have an almost linear orientation (Bogduk *et al.*, 1992a). (2) The maximum contractile stress in all muscles was assumed to be constant and equal to 460 kPa (Bogduk *et al.*, 1992a).

In order to analyze the static equilibrium of the model, the muscle attachment points were used to define the muscle force direction vector $\{t\}$ and the distance vector from the muscle attachment to the corresponding vertebral body center $\{r\}$ as defined in Fig. 3. Thus the six global components of force and moment $\{F_m\}$ of a single muscle about a vertebral body center are

$$\{F_m\} = \begin{Bmatrix} F \\ M \end{Bmatrix} = \begin{Bmatrix} T\{t\} \\ \{r\} \times T\{t\} \end{Bmatrix} = \begin{Bmatrix} \{t\} \\ \{r\} \times \{t\} \end{Bmatrix} T, \quad (1)$$

where T represents the magnitude of muscle tension.

The stiffness model was developed to incorporate published stiffness data for the six degrees of freedom of intervertebral motion segments. The displacements (translations and rotations) of the motion segments were variables in the model. The lumbar motion segments were represented by beam elements matched (Gardner-Morse *et al.*, 1990) to experimentally derived linear stiffness matrix data of Panjabi *et al.*, (1976) [Fig. 2(a)]. Equilibrium equations for small displacements take the form

$$\{F_v\} = [k]\{d\}, \quad (2)$$

where $[k]$ represents the motion segment beam stiffness matrix, $\{d\}$ the three displacements and three rotations of the two vertebrae of the motion segment, and $\{F_v\}$ the forces and moments at the vertebral body centers.

In the static model with a 'ball-and-socket' representation of motion segments, the joints could transmit forces but not moments. These joint forces became variables in place of the joint displacements. Each 'ball-and-socket' joint was assumed to be centered between two vertebral bodies [Fig. 2(b)]. The forces acting on a vertebra from these joint forces is represented by

$$\{F_j\} = \begin{Bmatrix} \{J\} \\ \{v\} \times \{J\} \end{Bmatrix}, \quad (3)$$

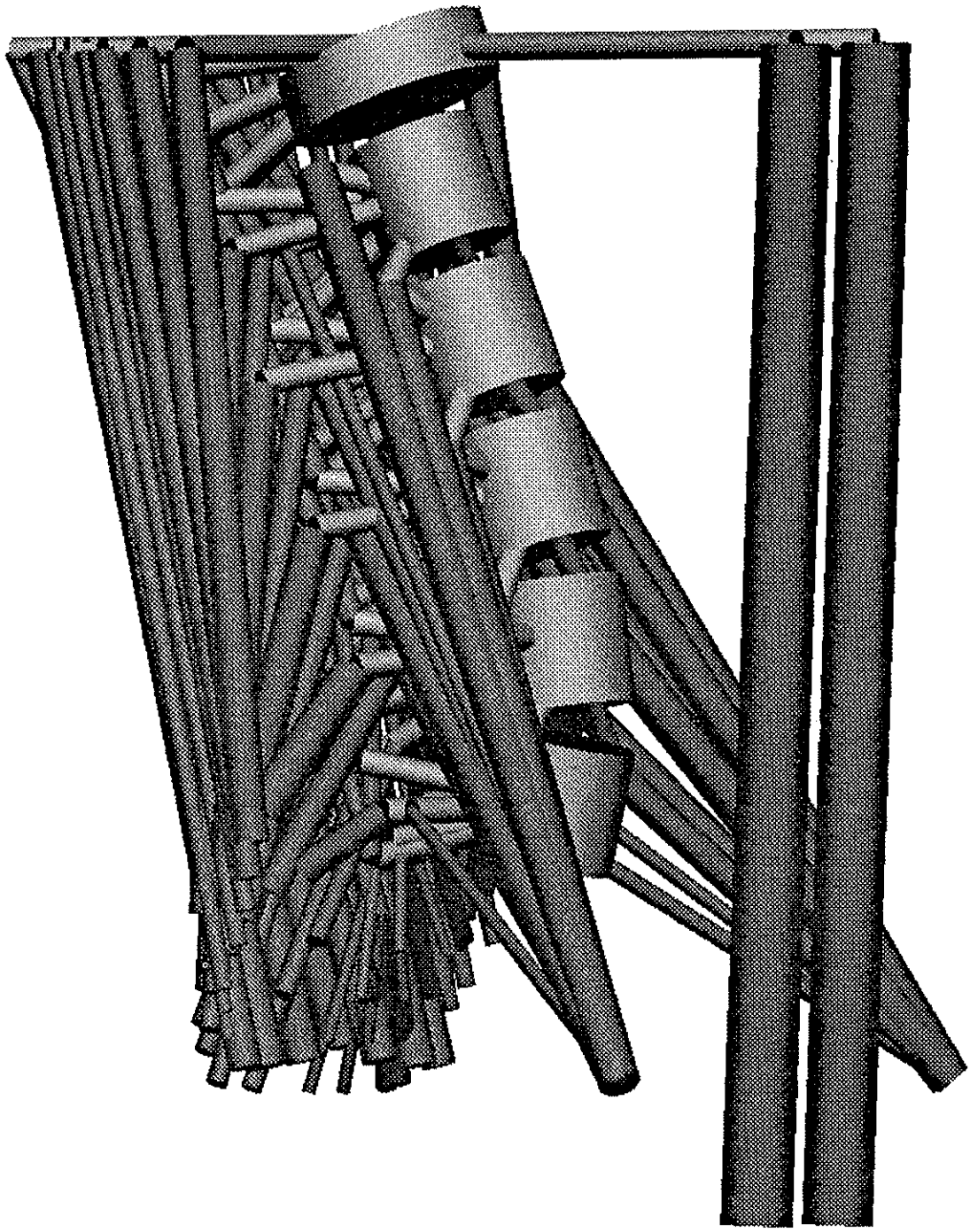

Fig. 1. Perspective (antero-lateral) view of the geometry of the model in which muscles are shown as cylinders with radii proportional to physiological cross sectional area. The vertebrae and vertebral extensions to the muscle attachment points are shown as lighter shaded cylinders. All attachments to the thorax are made to a single body at the top of the model. The pelvis and sacrum (which were considered to be fixed) are not represented in this image.

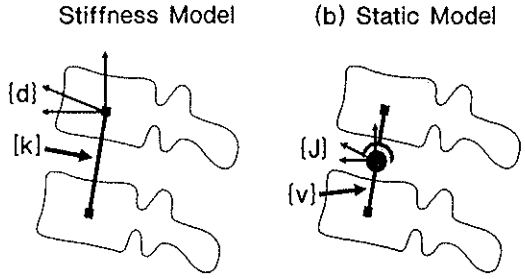

Fig. 2. Two representations of the motion segments in the models: (a) In the stiffness model, a beam with stiffness matrix $[k]$ transmits forces and moments, depending on the displacements $\{d\}$ of the vertebral body centers shown by squares. (b) In the static model, joint forces $\{J\}$, but no moments are transmitted through a 'ball-and-socket' joint positioned midway between the two vertebral centers.

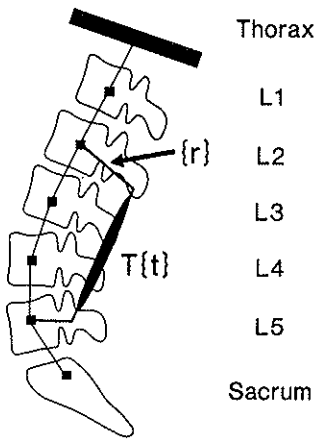

Fig. 3. Lateral view of lumbar spine model. The positions of vertebral body centers are shown by squares. A general muscle has a unit direction vector $\{t\}$ and is activated with tension T. Its vertebral attachment is identified relative to the vertebral body center by the vector $\{r\}$.

where $\{J\}$ represents the 'ball-and-socket' joint forces and $\{v\}$ the distance vector from the joint to the vertebral body center as shown in Fig. 2(b).

The rigid bodies representing the thorax and the vertebrae L1–L5 are in equilibrium when all the forces and moments at each vertebra are zero. The forces and moments consist of muscle forces, motion segment forces and applied external loads. There are six equilibrium equations for each of the five vertebrae and the thorax. The equilibrium equations take the form of equation (4) for the stiffness model and equation (5) for the static model.

$$\{F_M\}-[K]\{D\}+\{F_{EXT}\}=\{0\}, \quad (4)$$

$$\{F_M\}+\{F_J\}+\{F_{EXT}\}=\{0\}, \quad (5)$$

In these equations $\{F_M\}$ represents the forces from the 132 muscles, $\{F_J\}$ represents the forces from the six joints, $\{F_{EXT}\}$ represents the external forces acting on the thorax and the five lumbar vertebrae, $[K]$ represents the lumbar spine motion segment stiffness and $\{D\}$ represents the displacements of the thorax and vertebrae.

In these analyses the 132 muscle forces and either the six displacements at each vertebra or the three forces between each pair of vertebrae were considered as variables (168 or 150 variables). Linear programming was used to calculate these variables subject to constraints on spinal equilibrium, muscle stress and intervertebral displacements.

The objective function was the external loading and it was maximized in these analyses. Rather than attempting to simulate particular *in vivo* loading conditions, the model was used to analyze four moments individually applied at the vertebral body center of T12 in the thorax. Analyses were performed for extension, flexion, lateral bending or axial torque. The linear optimization was performed using the routine 'lp' in the optimization toolbox of Matlab (The MathWorks Inc., Natick, MA).

There were three sets of constraints: equilibrium, muscle stress and, for the stiffness model, intervertebral displacements. The lower constraint for all muscle forces was zero to prevent the muscles from going into compression. The upper constraint of muscle forces was such that the muscle stress did not exceed 460 kPa (Bogduk *et al.*, 1992a).

In the stiffness model the intervertebral displacements of vertebral body centers were constrained to be less than 5 mm and 5° in the sagittal plane and 2 mm and 2° in the other planes. Only axial displacements were unconstrained. These constraints were chosen to represent physiologic limits. The ranges of permitted rotations are smaller than the ranges of motion of lumbar spinal motion segments given by Panjabi *et al.*, (1989). These constraints also insure that the displacements are small as required by the assumption in equation (2).

The sensitivity of the objective function (maximum moment) to the motion segment stiffness and intervertebral displacement constraints were examined using dimensionless sensitivities:

$$\lambda=\frac{\Delta f}{\Delta P}\frac{P}{f}, \quad (6)$$

where λ represents the dimensionless sensitivity and $\Delta f/\Delta P$ the sensitivity of the objective function f to the parameter P which is the motion segment stiffness (k) or the intervertebral displacement constraint (D_v).

RESULTS

There were differences in both the magnitude of the maximum moments (efforts) which could be transmitted through the spine (Table 1), and in the pattern of recruitment of muscles (Table 2) for the models with and without motion segment stiffness. The stiffness model was associated with greater activation of mus-

Table 1. Predicted and published maximum efforts (N m)

	Extension effort	Flexion effort	Lateral bending effort	Axial torque effort
Static model*	44	12	11	3
Stiffness model*	63	23	25	10
Males†	189	143	141	97
Females†	102	89	75	60

*Maximum efforts about T12.

†Maximum efforts about L5–S1 for extension, flexion, and lateral bending are averages for subjects over 30 y of age from McNeill *et al.* (1980). Maximum axial torque values are from McGill and Hoodless (1990).

cles and different muscles being activated (Table 2). In both models many muscles were not active in maximum effort conditions. For extension efforts there were 35 active muscle pairs (of which 33 were maximally active) in the stiffness model and 27 active muscle pairs (of which 22 were maximally active) in the static model (Table 2). For maximum flexion efforts, the rectus abdominis was 100% active in the stiffness model, compared with only 86% active in the static model. In the stiffness model, three of four active muscle pairs were maximally active.

The maximum efforts (Table 1) were between 1.4 and 3.3 times greater in the stiffness model. For flexion efforts, the stiffness model produced 1.9 times greater moment than the static model and for extension effort, 1.4 times greater moment. The difference in moments between the models was greater than any moments transmitted through the motion segments in all loading directions (Table 3). Therefore, the difference was not due just to moments generated by the relative joint movements in the stiffness model. Also, the joint moments calculated in the stiffness model were very different at different levels of the spine.

Using the definition of an antagonistic muscle as one which was equally or more active for an effort in the opposite direction, there was a great deal of antagonistic muscle activity in the static model for nonsagittal plane efforts. (In Table 2 any muscle pair with activity on both sides is considered to have antagonistic activity because the model was symmetric.) Of the 13 active pairs in the static model, 11 could be considered as antagonists because these were muscles which were more or equally active in the extension effort. There were nine antagonistic muscles for lateral bending and six for axial torque (Table 2). The stiffness model retained some of this antagonistic activity (two antagonists) in lateral bending, but no antagonistic activity in axial torque.

Models which ignore the requirement for simultaneous equilibrium at all joints and maximally activate all synergistic muscles predict higher maximum efforts. To illustrate this we performed an analysis of a horizontal cutting plane through L3–L4, with maximal contraction of all synergistic muscles crossing that joint. The extension moment was equal to 125 N m, compared with 44 N m for the static model, and 63 N m for the stiffness model.

The maximum effort which could be generated by the stiffness model was dependent on both joint stiffness and the displacement constraints. The dimensionless sensitivities of the maximum efforts to motion segment stiffness ranged from 0.49 to 0.67 for the four loading directions. Thus, for a 2% change in joint stiffness, the maximum moment would have a corresponding change of approximately 1%.

Displacement constraints were reached only at a few vertebral levels. For extension efforts, three intervertebral displacements reached the limiting value specified in the constraints in the stiffness model. These were 5 mm of anterior displacement and 5° of flexion at T12–L1, and 5 mm of anterior displacement at L5–S1 (Table 4). The maximum extension effort was most sensitive to the displacement at L5, as evidenced by the sensitivity values given in Table 4.

DISCUSSION

In this study the equilibrium of the spine was analyzed in a model in which (1) equilibrium was respected simultaneously at all the joints of the lumbar spine, and (2) in which the motion segments had realistic stiffness properties. Both of these factors had a substantial effect on both the predicted maximum moments and pattern of muscle recruitment.

The requirement that all levels of the spine be in equilibrium simultaneously limited the number of active muscles and the degree of activation which could be achieved without violating equilibrium constraints. The inclusion of joints with stiffness (i.e. joints which could transmit both forces and moments) produced a model which predicted greater maximum external moments (efforts), along with a different pattern of muscle recruitment. Both models showed evidence of antagonistic muscle activity but there was less in the stiffness model. Antagonism is usually defined by reference to the moment of a muscle about a single joint (Andrews and Hay, 1983; Herzog and Binding, 1992). It is difficult to define antagonism in a multijoint system. Here we used the activation of a particular muscle in efforts in opposite directions as evidence of antagonism. Generally, only models with nonlinear cost functions predict antagonistic muscle activity (Herzog and Binding, 1992; Pedersen *et al.*, 1987). Herzog and Binding (1992) also demonstrated

Table 2. Simulated muscle forces as percent of physiologic maximum for extension, flexion, lateral bending and axial torque efforts for the static and stiffness models

Muscle name‡	Extension effort†		Flexion effort†		Lateral bending effort				Axial torque effort			
					Static model		Stiffness model		Static model		Stiffness model	
	Static model	Stiffness model	Static model	Stiffness model	Right	Left	Right	Left	Right	Left	Left	Right
tmf_L1	100	100	100	—	81	100	93	—	52	100	—	100
tmf_L2	100	100	100	—	13	100	—	—	—	100	—	100
tmf_L3	100	100	100	—	9	100	—	59	—	100	—	100
mf_L4	100	100	42	—	—	1	—	55	—	100	—	100
tmf_L5	—	100	—	—	—	—	—	—	—	100	—	100
m1s	100	100	—	—	—	15	—	—	—	—	—	—
m1t.1	—	100	—	—	—	—	—	—	—	—	—	—
m1t.2	—	—	—	—	—	—	—	—	—	—	—	—
m1t.3	—	—	—	—	—	—	—	—	—	—	—	—
i1	94	100	—	—	8	—	—	—	31	—	—	—
l1	—	73	—	—	—	—	—	—	—	—	—	—
m2s	—	100	—	—	—	—	—	—	—	—	—	—
m2t.1	—	—	—	—	—	—	—	—	—	—	—	—
m2t.2	100	100	—	—	—	—	—	—	—	—	—	—
m2t.3	100	100	—	—	—	—	—	—	—	1	—	—
i2	17	—	—	—	9	—	—	—	19	—	—	—
l2	100	100	—	—	—	—	—	—	—	—	—	—
m3s	—	—	—	—	—	—	—	—	—	—	—	—
m3t.1	—	100	—	—	—	—	—	—	—	—	—	—
m3t.2	—	100	—	—	—	—	—	—	—	—	—	—
m3t.3	—	100	—	—	—	—	—	—	—	—	—	—
i3	87	100	—	—	6	—	—	—	14	—	1	—
l3	—	100	—	—	—	—	—	—	—	—	—	—
m4s	—	—	—	—	—	—	—	—	—	—	—	—
m4t.1	—	100	—	—	—	—	—	—	—	—	—	—
m4t.2	—	100	—	—	—	—	—	—	—	—	—	—
m4t.3	—	—	—	—	—	—	—	—	—	—	—	—
i4	100	100	—	—	5	—	—	—	17	—	—	—
l4	80	100	—	—	—	—	—	—	—	26	—	—
m5s	100	—	100	—	100	100	—	—	100	100	—	—
m5t.1	100	100	100	—	100	100	—	—	100	100	—	—
m5t.2	100	100	100	—	100	100	—	—	100	100	—	—
m5t.3	100	—	100	—	100	100	—	—	100	100	—	—
l5	100	100	100	100	100	92	100	100	100	78	100	—
LT1	100	100	—	—	100	—	—	—	51	—	100	—
LT2	100	100	31	—	100	—	—	—	100	—	25	—
LT3	100	100	10	—	100	18	—	—	100	—	—	—
LT4	100	100	—	—	—	—	—	—	—	—	—	—

(*Continued*)

Table 2. Continued

Muscle name‡	Extension effort†		Flexion effort†		Lateral bending effort				Axial torque effort			
					Static model		Stiffness model		Static model		Stiffness model	
	Static model	Stiffness model	Static model	Stiffness model	Right	Left	Right	Left	Right	Left	Left	Right
LT5	100	100	—	—	36	—	—	—	10	—	—	—
LT6	—	100	—	—	—	—	—	—	—	—	—	—
LT7	—	—	—	—	—	—	—	—	—	—	—	—
LT8	—	—	—	—	—	—	—	—	—	—	—	—
LT9	—	—	—	—	—	—	—	—	—	—	100	—
LT10	3	9	—	—	—	—	—	—	—	—	—	—
LT11	100	100	—	—	—	—	—	—	—	—	—	—
LT12	100	100	—	—	—	—	95	—	—	—	—	38
IT5	100	100	—	—	—	—	100	—	—	—	—	—
IT6	—	—	—	—	—	—	100	—	—	—	—	—
IT7	—	—	—	—	—	—	100	—	—	—	—	—
IT8	—	—	—	—	—	—	100	—	—	100	—	100
IT9	—	—	—	—	—	—	100	—	—	100	—	100
IT10	—	—	—	—	52	—	100	—	—	63	—	100
IT11	—	—	—	—	100	—	100	—	—	—	—	—
IT12	—	—	—	—	100	—	100	—	—	—	100	—
pL1VB	—	—	—	—	—	—	—	—	—	—	—	37
pL1TP	—	—	—	—	—	—	—	—	—	—	—	—
pL1–L2IVD	—	—	—	100	3	—	31	—	2	—	—	56
pL2TP	—	—	—	—	—	83	—	—	—	63	—	100
pL2–L3IVD	—	—	42	11	—	—	98	57	—	—	35	—
pL3TP	—	—	—	—	—	39	—	—	—	33	—	54
pL3–L4IVD	—	—	—	—	—	—	—	—	—	—	—	—
pL4TP	—	—	—	—	—	—	—	—	—	28	—	—
pL4–L5IVD	—	—	—	—	—	—	—	—	—	—	—	—
pL5TP	—	—	—	—	16	—	—	—	—	68	—	—
pL5VB	—	—	—	—	—	—	—	—	—	—	—	—
RecAbdom	—	—	86	100	100	—	100	—	100	—	100	—

* All muscle forces are expressed as a percentage of the physiologic maximum based on their physiologic cross-sectional area (PCSA) and an assumed effective maximum muscle stress of 460 kPa (Bogduk *et al.*, 1992a).

† The muscle forces were symmetric so only the muscle forces for one side are given in the table.

‡ The muscle names are based on the notation of Bogduk *et al.*, 1992a, b. tmf = thoracic multifidus; m = multifidus; i = iliocostalis lumborum pars lumborum; l = longissimus thoracis pars lumborum; LT = longissimus thoracic; IT = iliocostalis lumborum pars thoracis; p = psoas major.

that models having multijoint muscles are more likely to predict antagonistic muscle activity. Here, it was apparently because of the predominance of multijoint muscles that a system with a linear cost function predicted antagonism.

The published experimental maximum moments for extension, flexion and lateral bending (Table 1) were greater than those found in this model. However, since it is difficult to apply pure moments about the spine *in vivo* the experimental moments were obtained by measuring a horizontal force applied to the chest, multiplied by the measured distance to L5–S1 (McNeill *et al.*, 1980). Based on typical dimensions of the trunk, the moments about T12 (where moment were applied in this model) would be between 50 and 70% of those at L5–S1. Taking this into account, the agreement was close for extension effort. For both models, moments in the other directions were underestimated. This difference could be due to the omission of the oblique abdominal muscles in the case of axial torque and omission of quadratus lumborum and the abdominal muscles in the case of lateral bending efforts. Also, posture was not controlled in the published experiments and subjects may have used a different (flexed) posture in which they could develop greater efforts than in the neutral posture simulated here. Another possible source of this difference could be that the PCSA values for this model were obtained from cadavers which may have atrophied muscles compared to the subjects in the experimental studies.

The model reported here shows that maximum contraction of all muscles would be inappropriate because it would violate joint equilibrium and cause large unbalanced moments and displacements of the spine. This observation suggests a possible mechanism for 'self-injury' of the spine through inappropriate contraction of the muscles.

Increasing either the motions segment stiffness or permitted motion was found to increase maximum efforts. This implies that changes in the stiffness of motion segments with age, injury or degeneration could result in substantial changes in the transmission of loads through the motion segments and the lumbar spine.

Table 3. Motion segment forces and moments in the stiffness model

	Forces			Moments*		
Level	Axial (N)	Sagittal shear (N)	Lateral shear (N)	Axial torque (N m)	Lateral bending (N m)	Flexion–Extension (N m)
Extension effort						
T12–L1	1014	−32	0	0	0	13
L1–L2	1118	43	0	0	0	9
L2–L3	1120	100	0	0	0	8
L3–L4	1323	181	0	0	0	0
L4–L5	1469	61	0	0	0	−4
L5–S1	1359	−458	0	0	0	4
Flexion effort						
T12–L1	439	201	0	0	0	8
L1–L2	624	191	0	0	0	1
L2–L3	830	153	0	0	0	−5
L3–L4	856	60	0	0	0	−8
L4–L5	844	−155	0	0	0	6
L5–S1	770	−482	0	0	0	2
Lateral bending effort						
T12–L1	627	143	11	5	−5	1
L1–L2	604	154	12	5	−5	−2
L2–L3	746	123	29	5	−4	−7
L3–L4	831	28	45	5	−2	−8
L4–L5	794	−170	48	5	−2	−5
L5–S1	718	−472	48	4	−2	3
Axial torque effort						
T12–L1	693	111	−43	5	5	−3
L1–L2	725	118	−58	5	3	−5
L2–L3	767	94	−66	5	1	−7
L3–L4	785	7	−59	5	−1	−8
L4–L5	730	−171	−53	5	−3	−4
L5–S1	605	−451	−32	3	−5	5

*Moments are referenced to the midpoint of the motion segment.

The model behavior was dependent on the bounds set for joint movement, because this limited the amount of shear force and moment transmission in the stiffness model. There is little experimental data about the *in vivo* forces or range of motion of lumbar motion segments. Here, the limits on joint displacements were referenced to the vertebral body centers. Thus rotations can contribute to the displacements, and the displacements of the vertebral body centers can be greater than the shear deformation of the discs, because of the finite offsets of the vertebral body centers from the disc. The relative 5 mm displacement constraint could be reached by relative rotation, by shearing across the disc, or a combination of both.

Rather than analyzing submaximal efforts, this study used maximum load as an objective function. This avoids the controversial issue of which physiologic cost function to use in an objective function to determine muscle recruitment strategy. Kuo and Zajac (1993) used a similar objective function in an analysis of walking in order to find which muscles tended to limit performance.

The model used a simplification of the true muscular anatomy. Most of these simplifications probably affected both models equally. Single joint intervertebral muscles (intertransversii and rotatores) were omitted because they are relatively small and close to the spine. The oblique and transverse abdominal muscles and quadratus lumborum were omitted because of the lack of detailed information on their three-dimensional anatomy. The main effect of these simplifications of anatomy is expected to be on lateral bending, axial rotation and possibly flexion efforts. Intraabdominal pressure effects (Morris *et al.*, 1961) and possible effects of the abdominal muscles on the thoracolumbar fascia (Gracovetsky *et al.*, 1985) were

Table 4. Intervertebral displacements (D_v) in the stiffness model as percent of constraints* with dimensionless constraint sensitivities (λ)†

		Extension effort 63 N m		Flexion effort 23 N m		Lateral bending effort 25 N m		Axial torque effort 10 N m	
Vertebral level	Degree of freedom	D_v (%)	λ	D_v (%)	λ	D_v (%)	λ	D_v (%)	λ
T12	Tx	−100	0.004	84	—	100	0.06	100	0.03
	Ty	—	—	—	—	100	0.003	−11	—
	Rx	—	—	—	—	−100	0.1	100	0.1
	Ry	−100	0.1	−64	—	−8	—	22	—
	Rz	—	—	—	—	−100	0.2	−100	0.5
L1	Tx	−41	—	100	0.3	100	0.001	85	—
	Ty	—	—	—	—	47	—	34	—
	Rx	—	—	—	—	−100	0.0002	64	—
	Ry	−73	—	−11	—	13	—	40	—
	Rz	—	—	—	—	−96	—	−100	0.008
L2	Tx	3	—	89	—	80	—	59	—
	Ty	—	—	—	—	2	—	63	—
	Rx	—	—	—	—	−73	—	12	—
	Ry	−65	—	36	—	51	—	52	—
	Rz	—		—	—	−97		−100	0.01
L3	Tx	36	—	45	—	32	—	14	—
	Ty	—	—	—	—	−17	—	75	—
	Rx	—	—	—	—	−38	—	−25	—
	Ry	0	—	60	—	63	—	59	—
	Rz	—	—	—	—	−100	0.03	−100	0.02
L4	Tx	4	—	−26	—	−34	—	−45	—
	Ty	—	—	—	—	−12	—	74	—
	Rx	—	—	—	—	−30	—	−67	—
	Ry	33	—	49	—	43	—	32	—
	Rz	—	—	—	—	−96	—	−97	—
L5	Tx	−100	0.6	−100	0.2	−100	0.04	−100	0.02
	Ty	—	—	—	—	−10	—	41	—
	Rx	—	—	—	—	−45	—	−100	0.005
	Ry	−33	—	−14	—	−22	—	−38	—
	Rz	—	—	—	—	−78	—	−51	—

*Tx = posterior displacement, Ty = displacement to the right, Tz (not constrained), Rx = left lateral bending, Ry = extension bending, Rz = counterclockwise axial rotation as seen from above.

†See equation (6) for the definition of λ.

not considered since it appears that these mechanisms have a relatively small effect on trunk biomechanics (McGill and Norman, 1986; MacIntosh *et al.*, 1987).

The maximum effective muscle stress was assumed to be the same for all muscles and equal to 460 kPa. In fact, maximum effective stress varies with muscle pennation and with muscle length relative to its resting length. Muscle pennation increases the force generated by a muscle at the expense of reduced shortening. Previous trunk models have assumed that maximum effective muscle stress lies in the range 100–900 kPa (Schultz, 1990), so the 460 kPa value used here represents a midrange value. Muscle length changes resulting from joint displacements in the stiffness model were small and were ignored.

Rather than assuming a line of action of forces in the motion segments, the stiffness model used experimentally determined properties. This is probably a simplification of the true nonlinear *in vivo* behavior of the motion segments. Panjabi *et al.* (1989) proposed that there is a 'neutral zone' in which the stiffness is negligible for small rotations, as was assumed in the static model. Since the results of this study demonstrate that moment transmission in the motion segments has a great effect on lumbar spinal load transmission, this points to the need to determine the true *in vivo* motion segment behavior. The small unisegmental muscles which were omitted from this model might also generate moments, thus augmenting the effect of joint moments due to stiffness found here.

It is interesting to note that there were both axial and lateral bending joint moments (Table 3) for the pure axial torque and lateral bending efforts. These moments were associated with coupled displacements. This was not the result of the motion segment stiffness properties because these were constant at all levels, while the pattern of coupled motion was different between levels. Also, the motion segment beams did not include coupling between lateral bending and axial rotations.

The widely used two-dimensional slice analyses of spinal forces assume that muscle forces only need to satisfy equilibrium at the one anatomic level under consideration. The findings of this study demonstrate that this is generally not compatible with equilibrium at other levels, since so many muscles of the lumbar spine cross multiple levels. The effect of moment transmission in the joints of the stiffness model was to increase the predicted maximal efforts and to bring them closer to published values, implying a more realistic representation of the lumbar spine. This also suggests that changes in motion segment stiffness with age, injury or degeneration would alter the pattern of muscle activation, and the trunk strength of an individual.

Acknowledgement—Supported by NIH R01 AR 40093 and PHS S07 05429 Biomedical Research Support Grant to the University of Vermont. We are most grateful to Professor Nikolai Bogduk for his generous assistance with providing data for muscular anatomy and Jim Tranowski for writing software used to create Fig. 1.

REFERENCES

Andersson, G. B. J. and Winters, J. M. (1990) Role of muscle in postural tasks: Spinal loading and postural stability. In *Multiple Muscle Systems: Biomechanics and Movement Organization* (Edited by Winters, M. J. and Woo, S. L. Y.) pp. 377–394. Springer, New York.

Andres, R. O. and Chaffin, D. B. (1991) Validation of a biodynamic model of pushing and pulling, *J. Biomechanics* **24,** 1033–1045.

Andrews, J. G. and Hay, J. G. (1983) Biomechanical considerations in the modeling of muscle function. *Acta Morphol. Neerl.-Scand.* **21,** 199–223.

Bergmark, A. (1989) Stability of the lumbar spine. A study in mechanical engineering. *Acta orthop. scand. Suppl.* **230,** 1–54.

Bogduk, N.(1993) Personal communication, 6th January 1993. The University of Newcastle, Newcastle, NSW 2308, Australia.

Bogduk, N., Macintosh, J. E. and Pearcy, M. J. (1992a) A universal model of the lumbar back muscles in the upright position, *Spine* **17,** 897–913.

Bogduk, N., Pearcy, M. and Hadfield, G. (1992b) Anatomy and biomechanics of psoas major. *Clin. Biomech.* **7,** 109–119.

Cheng, C. and Kumar, S. (1991) A three-dimensional static torso model for the six human lumbar joints. *Int. J. Ind. Ergonomics* **7,** 327–339.

Dietrich, M., Kedzior, K. and Zagrajek, T. (1990) Modeling of muscle action and stability of the human spine. In *Multiple Muscle Systems: Biomechanics and Movement Organization* (Edited by Winters, M. J. and Woo, S. L. Y.) pp. 451–460. Springer, New York.

Gardner-Morse, M. G., Laible, J. P. and Stokes, I. A. F. (1990) Incorporation of spinal flexibility measurements into finite element analysis. *J. biomech. Engng* **112,** 481–483.

Gracovetsky, S., Farfan, H. and Helleur, C. (1985) The abdominal mechanism. *Spine* **10,** 317–324.

Herzog, W. and Binding, P. (1992) Predictions of antagonistic muscular activity using nonlinear optimization. *Math. Biosci.* **111,** 217–229.

Kuo, A. D. and Zajac, F. E. (1993) A biomechanical analysis of muscle strength as a limiting factor in standing posture. *J. Biomechanics* **26** (Suppl. 1), 137–150.

Ladin, Z., Murthy, K. R. and De Luca, C. J. (1991) The effects of external bending moments on lumbar muscle force distribution. *J. biomech. Engng* **113,** 284–294.

Lavender, S. A., Tsuang, Y. H., Andersson, G. B., Hafezi, A. and Shin, C. C. (1992a) Trunk muscle coactivation: The effects of moment direction and moment magnitude. *J. orthop. Res.* **10,** 691–700.

Lavender, S. A., Tsuang, Y. H., Hafezi, A., Andersson, G. B., Chaffin, D. B., and Hughes, R. E. (1992b) Coactivation of the trunk muscles during asymmetric loading of the torso. *Hum. Factors* **34,** 239–247.

McGill, S. M. (1992) A myoelectrically based dynamic three-dimensional model to predict loads on lumbar spine tissues during lateral bending. *J. Biomechanics* **25,** 395–414.

McGill, S. M. and Hoodless, K. (1990) Measured and modelled static and dynamic axial trunk torsion during twisting in males and females. *J. biomed. Engng* **12,** 403–409.

McGill, S. M. and Norman, R. W. (1986) Partitioning of the L4–L5 dynamic moment into disc, ligamentous, and muscular components during lifting. *Spine* **11,** 666–677.

MacIntosh, J. E., Bogduk, N., and Gracovetsky, S. (1987) The biomechanics of the thoracolumbar fascia. *Clin. Biomech.* **2,** 78–83.

McNeill, T., Warwick, D., Andersson, G., and Schultz, A. (1980) Trunk strengths in attempted flexion, extension, and lateral bending in healthy subjects and patients with low-back disorders. *Spine* **6,** 529–538.

Morris, J. M., Lucas, D. B. and Bresler, M. S. (1961) The role

of the trunk in stability of the spine. *J. Bone Jt Surg. (Am)* **43,** 327–351.
Panjabi, M., Abumi, K., Duranceau, J. and Oxland, T. (1989) Spinal stability and inter-segmental muscle forces. A biomechanical model. *Spine* **14,** 194–200.
Panjabi, M. M., Brand, R. A. and White, A. A. (1976) Three-dimensional flexibility and stiffness properties of the human thoracic spine. *J. Biomechanics* **9,** 185–192.
Pedersen, D. R., Brand, R. A., Cheng, C. and Arora, J. S. (1987) Direct comparison of muscle force predictions using linear and nonlinear programming. *J. biomech. Engng* **109,** 192–199.
Reid, J. G. and Costigan, P. A. (1985) Geometry of adult rectus abdominis and erector spinae muscles. *J. orthop. Sports phys. Ther.* **6,** 278–280.
Schultz, A. B., Andersson, G. B. J., Haderspeck, K., Ortengren, R. and Nordin, M. (1982) Analysis and measurement of lumbar trunk loads in tasks involving bends and twists. *J. Biomechanics* **15,** 669–676.
Schultz, A. B. (1990) Biomechanical analyses of loads on the lumbar spine. In *The Lumbar Spine* (Edited by Weinstein, J. N. and Wiesel, S. W.) pp. 160–171. Saunders, Philadelphia.
Seroussi, R. E. and Pope, M. H. (1987) The relationship between trunk muscle electromyography and lifting moments in the sagittal and frontal planes. *J. Biomechanics* **20,** 135–146.
Wilder, D. G., Pope, M. H., Seroussi, R. E., Dimnet, J. and Krag, M. H. (1989) The balance point of the intervertebral motion segment: an experimental study. *Bull. Hosp. Jt Dis. Orthop. Inst.* **49,** 155–169.
Wynarsky, G. T. and Schultz, A. B. (1991) Optimization of skeletal configuration: Studies of scoliosis correction biomechanics. *J. Biomechanics* **24,** 721–732.
Yettram, A. L. and Jackman, M. J. (1980) Equilibrium analysis for the forces in the human spinal column and its musculature. *Spine* **5,** 402–411.
Yettram, A. L. and Jackman, M. J. (1982) Structural analysis for the forces in the human spinal column and its musculature. *J. biomed. Engng* **4,** 118–124.

APPENDIX A

DETAILS OF MODEL GEOMETRY

Table A1. Positions of vertebral body centers in global coordinates

Vertebra name	Global coordinates*		
	x (mm)	y (mm)	z (mm)
T12	−25.6	0.0	163.9
L1	−15.0	0.0	137.4
L2	−4.3	0.0	111.4
L3	6.1	0.0	84.0
L4	13.5	0.0	55.6
L5	13.6	0.0	26.5
S1	0.0	0.0	0.0

*The global coordinate system corresponds to x anterior, y to the left and z upwards. The values given were obtained by direct measurement from full-size original figures provided by personal communication with Professor Bogduk.

Table A2. Muscle names, PCSAs, muscle origins and insertions with vertebrae attachments

Muscle name*	PCSA (mm^2)	Global coordinates†			Vertebra(e) attachments	Global coordinates†			Vertebra attachments
		x (mm)	y (mm)	z (mm)		x (mm)	y (mm)	z (mm)	
tmf_L1	120.00	−67.5	9.8	163.9	T12	−51.5	14.1	136.5	L1
tmf_L2	120.00	−71.7	5.8	163.9	T12	−40.4	13.9	113.0	L2
tmf_L3	120.00	−74.8	−2.2	159.6	T12	−29.1	17.3	85.6	L3
tmf_L4	80.00	−69.5	2.2	146.4	T12	−20.8	19.5	59.8	L4
tmf_L5	40.00	−64.2	2.2	133.1	T12	−17.0	24.5	34.7	L5
m1s	40.00	−48.5	2.7	108.2	L1	−20.8	19.5	59.8	L4
m1t.1	42.00	−54.0	2.1	106.8	L1	−17.0	24.5	34.7	L5
m1t.2	36.00	−54.0	2.1	106.8	L1	−15.5	23.6	16.7	Sacrum/pelvis
m1t.3	60.00	−54.0	2.1	106.8	L1	−41.7	37.8	−6.2	Sacrum/pelvis
i1	108.00	−37.2	34.9	127.5	L1	−38.6	44.0	7.2	Sacrum/pelvis
l1	79.00	−40.1	18.5	128.2	L1	−37.1	42.9	−7.0	Sacrum/pelvis
m2s	39.00	−37.1	1.8	85.4	L2	−17.0	24.5	34.7	L5
m2t.1	39.00	−42.5	2.1	80.5	L2	−15.5	23.6	16.7	Sacrum/pelvis
m2t.2	49.50	−42.5	2.1	80.5	L2	−40.1	40.1	−13.8	Sacrum/pelvis
m2t.3	49.50	−42.5	2.1	80.5	L2	−39.8	39.8	−3.2	Sacrum/pelvis
i2	154.00	−27.8	41.4	103.4	L2	−31.5	47.8	17.2	Sacrum/pelvis
l2	91.00	−30.1	21.8	103.6	L2	−35.2	42.4	0.1	Sacrum/pelvis
m3s	54.00	−27.1	1.8	60.0	L3	−15.4	23.6	16.7	Sacrum/pelvis
m3t.1	52.33	−32.8	2.3	54.5	L3	−41.5	34.8	−23.7	Sacrum/pelvis
m3t.2	52.33	−32.8	2.3	54.5	L3	−43.1	36.3	−17.9	Sacrum/pelvis
m3t.3	52.33	−32.8	2.3	54.5	L3	−43.1	37.5	−12.8	Sacrum/pelvis
i3	182.00	−16.1	42.8	76.8	L3	−27.5	49.9	22.2	Sacrum/pelvis
l3	103.00	−19.8	24.2	77.5	L3	−32.1	41.5	6.1	Sacrum/pelvis
m4s	46.50	−21.7	1.5	38.3	L4	−24.3	28.2	2.0	Sacrum/pelvis
m4t.1	46.50	−27.9	1.2	35.1	L4	−39.5	25.4	−24.7	Sacrum/pelvis
m4t.2	46.50	−27.9	1.2	35.1	L4	−35.9	26.7	−16.0	Sacrum/pelvis
m4t.3	46.50	−27.9	1.2	35.1	L4	−31.1	28.0	−7.6	Sacrum/pelvis
i4	189.00	−8.8	40.8	51.8	L4	−22.6	51.2	25.6	Sacrum/pelvis
l4	110.00	−10.8	25.1	51.4	L4	−27.5	39.4	11.1	Sacrum/pelvis
m5s	22.50	−21.2	1.9	20.3	L5	−17.5	8.8	0.1	Sacrum/pelvis
m5t.1	22.50	−26.2	1.9	16.8	L5	−38.0	6.4	−25.4	Sacrum/pelvis
m5t.2	22.50	−26.2	1.9	16.8	L5	−33.5	7.6	−16.1	Sacrum/pelvis
m5t.3	22.50	−26.2	1.9	16.8	L5	−26.0	8.3	−8.3	Sacrum/pelvis
l5	116.00	−8.8	30.1	25.2	L5	−22.8	35.9	14.7	Sacrum/pelvis

(*Continued*)

Table A2. Continued

Muscle name*	PCSA (mm^2)	Global coordinates†			Vertebra(e) attachments	Global coordinates†			Vertebra attachments
		x (mm)	y (mm)	z (mm)		x (mm)	y (mm)	z (mm)	
LT1	29.00	−83.9	2.8	163.9	T12	−55.1	0.4	98.9	L2
LT2	57.00	−97.1	4.9	163.9	T12	−54.8	1.6	83.3	L2
LT3	56.00	−87.8	5.6	163.9	T12	−40.3	1.3	58.3	L3
LT4	45.00	−88.2	4.3	163.9	T12	−37.0	1.2	46.7	L4
LT5	44.00	−96.3	8.2	163.9	T12	−36.8	1.5	42.5	L4
LT6	64.00	−89.8	5.7	163.9	T12	−34.2	1.8	25.1	L5
LT7	78.00	−73.9	7.2	163.9	T12	−26.0	1.9	6.6	Sacrum/pelvis
LT8	125.00	−76.1	13.9	163.9	T12	−30.4	1.1	−8.6	Sacrum/pelvis
LT9	146.00	−78.8	19.7	163.9	T12	−34.4	1.2	−16.9	Sacrum/pelvis
LT10	160.00	−78.7	22.8	163.9	T12	−34.4	14.2	−19.7	Sacrum/pelvis
LT11	167.00	−78.8	25.7	163.9	T12	−34.4	28.4	−20.7	Sacrum/pelvis
LT12	138.00	−78.7	29.1	163.9	T12	−34.4	36.6	−20.8	Sacrum/pelvis
IT5	23.00	−74.4	32.1	163.9	T12	−36.2	39.8	−15.3	Sacrum/pelvis
IT6	31.00	−72.5	35.6	163.9	T12	−35.1	43.0	−10.6	Sacrum/pelvis
IT7	39.00	−71.0	39.0	163.9	T12	−33.6	46.0	−6.3	Sacrum/pelvis
IT8	34.00	−66.5	42.4	163.9	T12	−29.2	48.5	1.4	Sacrum/pelvis
IT9	50.00	−62.0	43.6	163.9	T12	−25.6	51.9	7.7	Sacrum/pelvis
IT10	100.00	−55.9	48.7	163.9	T12	−23.1	55.1	13.5	Sacrum/pelvis
IT11	123.00	−46.5	52.0	163.9	T12	−20.6	58.4	20.0	Sacrum/pelvis
IT12	147.00	−35.6	55.2	163.9	T12	−19.9	61.5	25.7	Sacrum/pelvis
pL1VB	211.00	−29.9	16.3	141.8	L1	57.8	61.9	−24.1	Sacrum/pelvis
pL1TP	40.67	−34.8	19.1	128.2	L1	57.8	61.9	−24.1	Sacrum/pelvis
pL1–L2IVD	211.00	−14.4	18.1	119.9	L1 and L2	57.8	61.9	−24.1	Sacrum/pelvis
pL2TP	84.17	−24.4	23.4	103.1	L2	57.8	61.9	−24.1	Sacrum/pelvis
pL2–L3IVD	161.00	−0.9	19.9	91.0	L2 and L3	57.8	61.9	−24.1	Sacrum/pelvis
pL3TP	173.00	−13.2	30.0	76.5	L3	57.8	61.9	−24.1	Sacrum/pelvis
pL3–L4IVD	191.00	8.8	21.4	57.7	L3 and L4	57.8	61.9	−24.1	Sacrum/pelvis
pL4TP	120.00	−5.7	26.1	51.0	L4	57.8	61.9	−24.1	Sacrum/pelvis
pL4–L5IVD	119.00	11.8	21.6	31.3	L4 and L5	57.8	61.9	−24.1	Sacrum/pelvis
pL5TP	24.00	−1.2	33.3	25.3	L5	57.8	61.9	−24.1	Sacrum/pelvis
pL5VB	39.50	8.4	20.1	16.1	L5	57.8	61.9	−24.1	Sacrum/pelvis
Rec Abdom	525.00	45.0	15.0	163.9	T12	33.5	15.0	−75.0	Sacrum/pelvis

*The muscle names are based on the notation of Bogduk *et al.*, 1992a, b. tmf = thoracic multifidus; m = multifidus; i = iliocostalis lumborum pars lumborum; l = longissimus thoracis pars lumborum; LT = longissimus thoracic; IT = iliocostalis lumborum pars thoracis; p = psoas major.

†The global coordinate system corresponds to x anterior, y to the left and z upwards. The muscles are symmetric about the sagittal (x–z) plane so only the coordinates of the muscles for the left side are given in the table. The coordinates of the muscles for the right-hand side can be determined from the table by reversing the sign of the y-coordinate.